

**AN OPTICAL MODEL DESCRIPTION OF MOMENTUM TRANSFER
IN HEAVY ION COLLISIONS**

F. Khan and G. S. Khandelwal
Physics Department
Old Dominion University
Norfolk, VA 23529-0116 USA

and

L. W. Townsend and J. W. Wilson
NASA Langley Research Center
Hampton, VA 23665-5225 USA

and

J. W. Norbury
Department of Mathematics & Physics
Rider College
Lawrenceville, NJ 08648 USA

ABSTRACT

An optical model description of momentum transfer in relativistic heavy ion collisions, based upon composite particle multiple scattering theory, is presented. The imaginary component of the complex momentum transfer, which comes from the absorptive part of the optical potential, is identified as the longitudinal momentum downshift of the projectile. Predictions of fragment momentum distribution observables are made and compared with experimental data. Use of the model as a tool for estimating collision impact parameters is discussed.

1. INTRODUCTION

Since the pioneering experiments on relativistic heavy ion fragmentation using carbon and oxygen beams,^{1, 2} attention has been directed toward understanding the underlying mechanisms of fragmentation processes. Over the past two decades, a substantial body of literature has resulted from studies of these phenomena, and several excellent reviews have been written.³⁻⁶ Perhaps the most significant findings of the early experiments were the observations that the fragment momentum distributions were Gaussian in the projectile rest frame, and that the isotopic production cross sections factored into a product of target and beam-fragment terms. Initial attempts to explain these phenomena utilized a statistical model to describe the reactions.⁷⁻⁹ This later evolved into a two-step model called

abrasion-ablation¹⁰ where the abrasion stage can be formulated using geometric^{10,11} or quantum mechanical arguments.^{12, 13} In the present work, we use the impulsive excitation energy ideas of Fricke,¹⁴ within the context of composite particle multiple scattering theory, to derive a method for predicting momentum transfers occurring in relativistic heavy ion collisions. This momentum transfer is a function of impact parameter. A new feature of this work is that the momentum transfer is a complex quantity. The real component is the usual transverse momentum transfer resulting from elastic scattering. The imaginary component is explicitly shown to be the longitudinal momentum transfer, or downshift, arising from the absorptive part of the complex optical potential. Using this formalism, projectile nucleus fragment momentum "downshifts" resulting from the dynamics of the nuclear collision can be calculated and compared with laboratory beam measurements. In addition, modifications to the widths of the momentum distributions can be estimated using the formalism.

The outline of the paper is as follows. In section 2 the dynamical momentum transfer expression is derived, and representative calculations of momentum transfer as a function of impact parameter are presented. In section 3 the connections between collisional momentum transfer and fragment momentum downshifts/widths are made. A method of choosing appropriate impact parameters

for each fragmentation channel is then described. Next, calculations of momentum downshifts for fragments produced by oxygen nuclei colliding with various targets are made and compared with experimental data.² We also compute widths of momentum distributions for ^{139}La fragments and compare with recent experimental measurements.¹⁶ In section 4 we propose a method for using the momentum transfer model to estimate collision impact parameters. Finally, in section 5 we conclude by summarizing the current status of model development and discuss future directions for research.

2. METHOD OF CALCULATION

In reference 17, a coupled-channels Schrödinger equation for composite particle scattering, which relates the entrance channel to all of the excited states of the target and projectile, was derived by assuming large incident projectile kinetic energies and closure of the accessible eigenstates. The equation is written as

$$\left(\nabla^2 + k^2\right) \psi_{n\mu}(\vec{x}) = 2m A_p A_T (A_p + A_T)^{-1} \sum_{n'\mu'} V_{n\mu, n'\mu'}(\vec{x}) \psi_{n'\mu'}(\vec{x}) \quad (1)$$

where the subscripts n and μ (primed and unprimed) label the projectile and target eigenstates; m is the nucleon mass; A_p and A_T are the mass numbers of the projectile and target; \vec{k} is the projectile momentum relative to the center of mass; and \vec{x} is the projectile position vector relative to the target. In terms of the nucleon-

nucleon scattering t-matrix $t_{\alpha j}$, and the internal state vectors of the projectile $g_n^P(\vec{\xi}_p)$ and target $g_\mu^T(\vec{\xi}_T)$, it was also demonstrated that the potential matrix is expressible as

$$V_{n\mu, n'\mu'}(\vec{x}) = \left\langle g_n^P g_\mu^T \left| V_{\text{opt}}(\vec{\xi}_P, \vec{\xi}_T, \vec{x}) \right| g_{n'}^P g_{\mu'}^T \right\rangle \quad (2)$$

where

$$V_{\text{opt}}(\vec{\xi}_P, \vec{\xi}_T, \vec{x}) = \sum_{\alpha j} t_{\alpha j} \quad (3)$$

This same formalism can be used to investigate heavy ion collision momentum transfers. Within the context of eikonal scattering theory, the solution to the Schrödinger equation

$$H \Psi(\vec{x}, \vec{\xi}_P, \vec{\xi}_T) = E \Psi(\vec{x}, \vec{\xi}_P, \vec{\xi}_T) \quad (4)$$

is

$$\Psi(\vec{x}, \vec{\xi}_P, \vec{\xi}_T) = (2\pi)^{-3/2} \exp \left[-\frac{i}{v} \int_{-\infty}^z V_{\text{opt}}(\vec{x}, \vec{\xi}_P, \vec{\xi}_T) dz' \right] g_n^P(\vec{\xi}_P) g_\mu^T(\vec{\xi}_T) e^{i\vec{k} \cdot \vec{x}} \quad (5)$$

where v is the velocity. The total momentum of the projectile is then given by the matrix element involving the sum of the projectile single-nucleon momentum operators as

$$\vec{P}_{\text{tot}} = \left\langle \Psi \left| -i \sum_{\alpha=1}^{A_P} \vec{\nabla}_{P, \alpha} \right| \Psi \right\rangle \quad (6)$$

where the subscript P on the gradient operator denotes that the gradient is to be

taken with respect to the projectile internal coordinates. Equation (6) actually denotes a potential matrix $\vec{P}_{n\mu, n'\mu'}$ in analogy with (2). Therefore, substituting (5) into (6) yields

$$\vec{P}_{n\mu, n'\mu'} = \left\langle g_n^P(\vec{\xi}_P) g_{\mu}^T(\vec{\xi}_T) \left| e^{-iS} \left(-i \sum_{\alpha=1}^{A_P} \vec{\nabla}_{P, \alpha} \right) e^{iS} \right| g_{n'}^P(\vec{\xi}_P) g_{\mu'}^T(\vec{\xi}_T) \right\rangle \quad (7)$$

where

$$S = \frac{1}{v} \int_{-\infty}^z V_{opt}(\vec{x}', \vec{\xi}_P, \vec{\xi}_T) dz'. \quad (8)$$

Equation (7) can be further expressed as

$$\vec{P}_{n\mu, n'\mu'} = \vec{P}_0 + \left\langle g_n^P g_{\mu}^T \left| \left(- \sum_{\alpha}^{A_P} \vec{\nabla}_{P, \alpha} S \right) \right| g_{n'}^P g_{\mu'}^T \right\rangle \quad (9)$$

where the momentum before the collision is

$$\vec{P}_0 = \left\langle g_n^P g_{\mu}^T \left| \left(-i \sum_{\alpha=1}^{A_P} \vec{\nabla}_{P, \alpha} \right) \right| g_{n'}^P g_{\mu'}^T \right\rangle. \quad (10)$$

The total momentum transfer to the projectile is then given by

$$\vec{Q} = \vec{P}_{n\mu, n'\mu'} - \vec{P}_0 = \left\langle g_n^P g_{\mu}^T \left| \left(- \sum_{\alpha} \vec{\nabla}_{P, \alpha} S \right) \right| g_{n'}^P g_{\mu'}^T \right\rangle \quad (11)$$

For scattering near the forward directions, the couplings between various excited states is small and the off-diagonal elements in Eq. (11) can be neglected; hence, the

momentum transfer can be approximated by

$$\vec{Q} \approx \vec{P}_{e1} - \vec{P}_0 = \left\langle \begin{pmatrix} g_o^P & g_o^T \end{pmatrix} \left(- \sum_{\alpha} \vec{\nabla}_{P, \alpha} S \right) \begin{pmatrix} g_o^P & g_o^T \end{pmatrix}^T \right\rangle. \quad (12)$$

In terms of projectile and target number densities, and the constituent-averaged two-nucleon transition amplitude,¹⁸ \tilde{t} , Eq. (12) becomes

$$\vec{Q}(\vec{b}) = -A_P A_T \int d^3 \xi_P \rho_P(\xi_P) \int d^3 \xi_T \rho_T(\xi_T) \left[\vec{\nabla}_P \int_{-\infty}^{\infty} \tilde{t}(\vec{b} + \vec{z}' + \vec{\xi}_P - \vec{\xi}_T) \frac{dz'}{v} \right] \quad (13)$$

where the integration limit in the longitudinal direction has been extended to infinity. The momentum transfer in (13) is therefore only a function of the impact parameter of the collision. The projectile and target number densities (ρ_P and ρ_T) are normalized to unity as

$$\int \rho(\vec{x}) d^3 x = 1. \quad (14)$$

The constituent-averaged two-nucleon transition amplitude is obtained from the first-order t-matrix used in our previous studies¹³ of nucleus-nucleus collisions as

$$\tilde{t}(e, \vec{x}) = -(\epsilon/m)^{1/2} \sigma(e) [\alpha(e) + i] [2\pi B(e)]^{1/2} \exp \left[-x^2/2B(e) \right] \quad (15)$$

where e is the two-nucleon kinetic energy in their center-of-mass frame, $\sigma(e)$ is the nucleon-nucleon total cross section, $\alpha(e)$ is the ratio of the real-to-imaginary part of

the forward scattering amplitude, and $B(e)$ is the nucleon-nucleon slope parameter. Values for these parameters taken from various compilations are listed in reference 18.

The dynamical momentum transfer to the projectile, given by Eq. (13), results from interactions with the target. A new feature, unique to this work, is that it is a complex quantity. The real part of the momentum transfer, which comes from the real part of the complex optical potential, is the contribution arising from elastic scattering. It is purely transverse. The imaginary component, which comes from the absorptive part of the complex optical potential, is the longitudinal kinetic momentum downshift. To demonstrate this last assertion, we rewrite Eq. (13) symbolically as

$$\vec{Q} = (Q_R + iQ_I) \hat{b} \quad (16)$$

where i is $\sqrt{-1}$ and \hat{b} is the unit vector transverse to the beam direction. If \hat{z} denotes the unit vector in the incident beam direction, then from elementary complex analysis¹⁹ we know that

$$i\hat{b} = -\hat{z} \quad (17)$$

since i is an operator which rotates a unit vector counterclockwise through $\pi/2$ radians. Therefore, the momentum transfer is

$$\vec{Q} = Q_R \hat{b} - Q_I \hat{z} \quad (18)$$

which we relabel for clarity as

$$\vec{Q} = Q_{\perp} \hat{b} - Q_{||} \hat{z}. \quad (19)$$

Note the similarity of this argument to that of complex indices of refraction in electromagnetic wave propagation. From Eq. (13), the transverse component is

$$\vec{Q}_{\perp} = -A_P A_T \int d^3 \xi_P \rho_P(\vec{\xi}_P) \int d^3 \xi_T \rho_T(\vec{\xi}_T) \vec{\nabla}_P \int_{-\infty}^{\infty} \text{Re } i \left(\vec{b} + \vec{z}' + \vec{\xi}_P - \vec{\xi}_T \right) \frac{dz'}{v} \quad (20)$$

and the longitudinal component is

$$Q_{||} = -A_P A_T \int d^3 \xi_P \rho_P(\vec{\xi}_P) \int d^3 \xi_T \rho_T(\vec{\xi}_T) \vec{\nabla}_P \int_{-\infty}^{\infty} \text{Im } i \left(\vec{b} + \vec{z}' + \vec{\xi}_P - \vec{\xi}_T \right) \frac{dz'}{v} \quad (21)$$

Calculated momentum transfers obtained using equations (20) and (21) are displayed in Figure 1 for ^{16}O at 2.1 AGeV colliding with a beryllium target. These calculations utilize the harmonic well nuclear densities from our previous work.^{13, 18} From the figure, two features are readily apparent. First, the longitudinal momentum transfer is larger than the transverse indicating the primarily absorptive nature of the nuclear collision at this energy. Second, the predicted momentum transfers decrease rapidly with increasing impact parameter. This will be a subject of further discussion in subsequent sections of this paper.

3. RESULTS

The collisional momentum transfers computed using the model described in the previous section can be related to experimentally-measured, heavy-ion fragment momentum downshifts/widths through considerations of energy and momentum conservation. As has been pointed out elsewhere,^{8, 20} a momentum transfer in any direction Q_j modifies the width h_j of the momentum distribution in that direction by

$$(h'_j)^2 = h_j^2 + \frac{F^2 Q_j^2}{A^2} \quad (22)$$

and the mean by

$$\vec{P}'_j = \vec{P}_j + \frac{F}{A} \vec{Q}_j. \quad (23)$$

From the latter, the longitudinal momentum downshift is given by

$$\Delta P_{||} = P'_{||} - P_{||} = \frac{F}{A} Q_{||} \quad (24)$$

where $Q_{||}$ is the magnitude of the longitudinal momentum transfer [obtained from eq. (21)], F is the fragment mass number, and A is the initial mass number of the fragmenting nucleus. Recalling that $Q_{||}$ is a function of impact parameter, an appropriate method for choosing it for each fragmentation channel is necessary. Recently a semiempirical abrasion-ablation fragmentation model, NUCFRAG, was proposed.²¹ Although it assumes simple uniform density distributions for the

colliding ions, and a zero-range (delta function) interaction, it does include frictional-spectator-interactions (FSI) and agrees with experimental cross section data to the extent that they agree among themselves. Also, and most importantly for this work, it is easily modified to yield the impact parameters for each fragmentation channel. Hence, the procedure for evaluating equations (22) and (24) is to extract impact parameters from NUCFRAG for each nucleon removal corresponding to $\Delta A = 1, 2, 3, \dots$. These impact parameters are then inserted into Eqs. (20) and (21) to obtain the corresponding momentum transfers for use in evaluating Eqs. (22) and (24). Because NUCFRAG uses uniform densities, uniform densities are also used in evaluating (20) and (21). In addition, the zero-range interaction in NUCFRAG is simulated for numerical integration purposes in (20) and (21) through the use of a very narrow Gaussian form for the t-matrix given by eq. (15). This narrow Gaussian is the same width for all collision pairs and therefore is not an arbitrarily adjusted parameter.

Representative calculations for momentum downshifts as a function of fragment mass number are displayed in Figure 2 for ^{16}O projectiles at 2.1 AGeV colliding with targets of Be, C, Al, Cu, Ag, and Pb. These momentum downshifts are target-averaged using simple arithmetic averaging. For comparison, the target-averaged experimental data from reference 2 are also displayed. For display and

comparison purposes, the latter are also averaged over all isotopes contributing to each fragment mass number using

$$(\Delta P_{||})_{\text{ave}} = \frac{\sum_i \sigma_i (\Delta P_{||}^i)_{\text{expt}}}{\sum_i \sigma_i} \quad (25)$$

where σ_i is the experimental production cross section for the i th fragment isotope. Comparing the theoretical estimates to the experimental data, reasonable agreement is obtained considering the simplified form of the nuclear fragmentation model used in the calculations and the overall sensitivity of the calculated momentum transfer to the choice of impact parameter. Improved agreement is expected if impact parameters from a fragmentation model using realistic nuclear densities and interactions were available. This is especially true for collisions involving lighter ions, such as carbon, oxygen, and beryllium, which are poorly represented by simple uniform nuclear distributions.

Figure 3 displays transverse momentum widths as a function of fragment mass number for 1.2 AGeV ^{139}La fragmenting in carbon targets. The experimental data are taken from reference 16. Again, impact parameters from NUCFRAG are used as inputs into the momentum transfer expressions [Eqs. (20) and (21)]. For consistency with the use of these impact parameters, a narrow Gaussian t -matrix and uniform nuclear densities were again utilized in the momentum transfer

calculations. From Figure 3, it is clear that the agreement is much better than in Figure 2 and probably reflects the fact that a uniform nuclear density distribution is a more reasonable approximation for a heavy nucleus-like lanthanum than for light nuclei such as oxygen.

4. ESTIMATING COLLISION IMPACT PARAMETERS

Thus far in this work, we have used collision impact parameters as inputs into a momentum transfer computational model which in turn has yielded estimates of heavy ion fragment momentum downshifts/widths for comparison with experimental data. However, this procedure can be reversed and the model used to estimate collision impact parameters from measured momentum downshifts for relativistic collisions. Let F be the fragment mass number with measured longitudinal momentum downshift $\Delta P_{||}$ produced in a relativistic collision between a projectile nucleus (mass number A) and some target. Then, from eq. (24), the longitudinal momentum transfer to the projectile from the target is

$$Q_{||} = \frac{A}{F} \Delta P_{||}. \quad (26)$$

The collision impact parameter can then be estimated from eq. (21) by computing $Q_{||}$ as a function of impact parameter (e.g., in Figure 1) and using $Q_{||}$ from eq. (26) as the entry. To illustrate, consider a collision involving 2.1 AGeV oxygen colliding

with a beryllium target. The calculated momentum transfer using realistic nuclear densities are displayed in Figure 1. If the measured (hypothetical) momentum downshift for the ^{14}N fragment is 35 ± 7 MeV/c, then eq. (26) yields a longitudinal momentum downshift of 40 ± 8 MeV/c. From Figure 1, the corresponding range of impact parameters is 6.1 - 6.4 fm. A similar procedure incorporating measured momentum distribution widths and Eqs. (22) and (20) or (21) could also be used to estimate collision impact parameters.

5. CONCLUDING REMARKS

Beginning with composite particle multiple scattering theory, an optical model description of collision momentum transfer in relativistic heavy ion collisions was derived. General expressions for transverse and longitudinal momentum transfer, which utilize a finite-range two-nucleon interaction and relativistic nuclear densities, were presented. The theory was used to estimate heavy ion fragment momentum downshifts for relativistic oxygen and transverse momentum widths for relativistic lanthanum projectiles. The main new feature of this work was the identification of the imaginary component of the momentum transfer as the longitudinal collision momentum transfer. Finally, the use of the model as a mechanism for estimating collision impact parameters was described.

The present theory is mainly applicable at intermediate or high energies because of the use of eikonal wavefunctions and the impulse approximation. At lower energies (below several hundred MeV/nucleon), the validity of straight line

trajectories and the assumption of a constant projectile velocity is questionable. Therefore, to compare theory with experiment at lower energies²² revisions to the model are necessary. In particular, deceleration corrections to the constant velocity assumption are being developed. For incident energies greater than 1 AGeV, first-order deceleration corrections are small (< 1 percent). As the incident energy decreases, however, the first-order corrections increase significantly (over 50 percent at 100 A MeV), indicating that higher-order terms must be included. Work on this is in progress and will be reported when completed.

The authors wish to thank Hank Crawford and Peter Lindstrom of Lawrence Berkeley Laboratory, and Frank Cucinotta of the Environmental Measurements Laboratory (USDOE) for useful comments and suggestions. This work was supported by NASA Grant Nos. NCCI-42 (F. K. and G. S. K.) and NAG-1-797 (J. W. N.)

REFERENCES

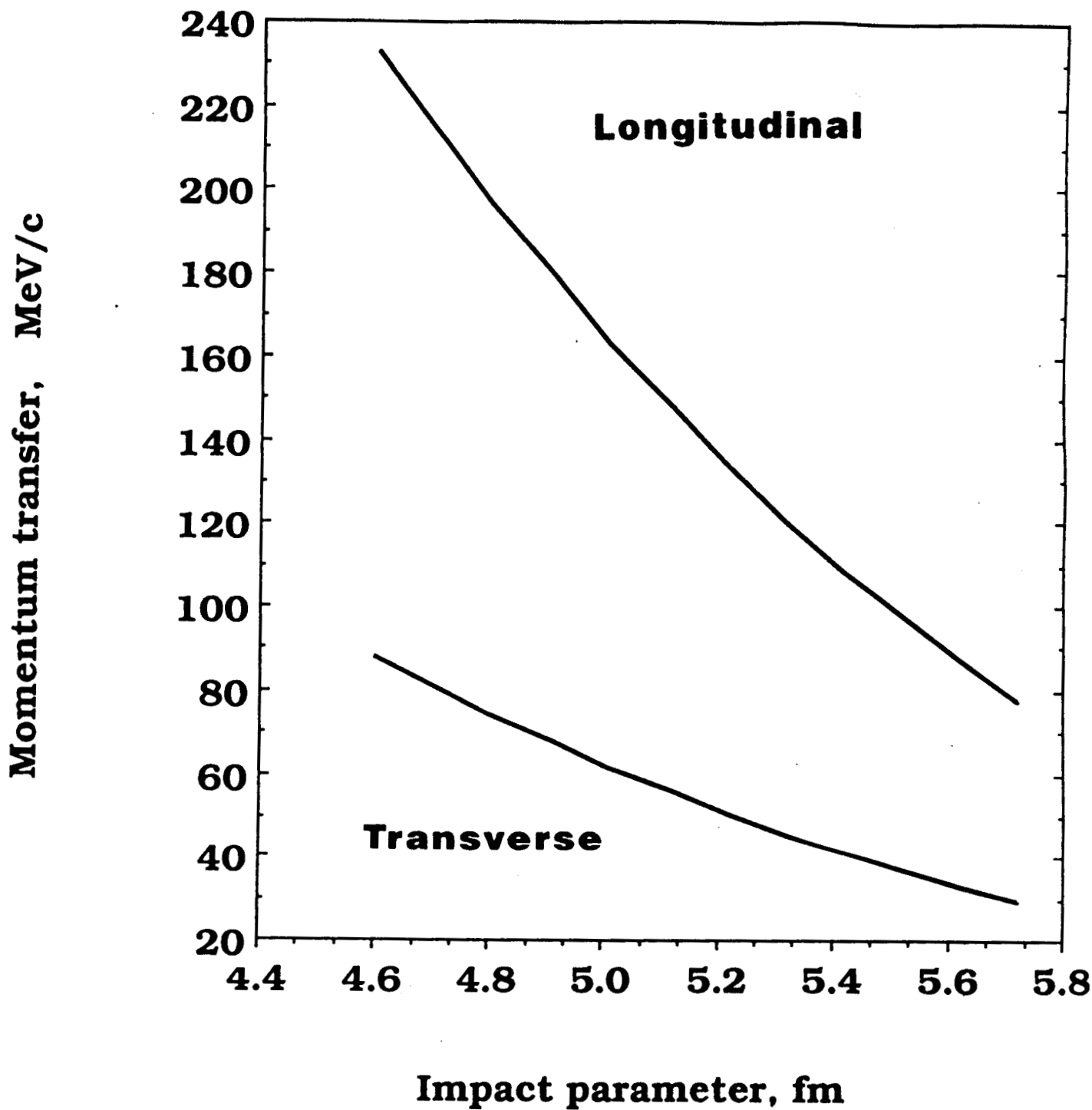
- ¹ P. J. Lindstrom, D. E. Greiner, H. H. Heckman, Bruce Cork, and F. S. Bieser, Lawrence Berkeley Laboratory Report No. LBL-3650, 1975 (unpublished).
- ² D. E. Greiner, P. J. Lindstrom, H. H. Heckman, Bruce Cork, and F. S. Bieser, Phys. Rev. Lett. 35 (1975) 152.
- ³ A. S. Goldhaber and H. H. Heckman, Ann. Rev. Nucl. Part. Sci. 28 (1978) 161.
- ⁴ S. Nagamiya, J. Randrup, and T. J. M. Symons, Ann. Rev. Nucl. Part. Sci. 34 (1984) 155.
- ⁵ J. Hufner, Phys. Rep. 125 (1985) 129.
- ⁶ G. Baur, F. Rösel, D. Trautmann, and R. Shyam, Phys. Rep. 111 (1984) 333.
- ⁷ H. Feshbach and K. Huang, Phys. Lett. 47B (1973) 300.
- ⁸ A. S. Goldhaber, Phys. Lett. 53B (1974) 306.
- ⁹ R. K. Bhaduri, Phys. Lett. 50B (1974) 211.
- ¹⁰ J. D. Bowman, W. J. Swiatecki, and C. F. Tsang, Lawrence Berkeley Laboratory Report No. LBL-2908, 1973 (unpublished).
- ¹¹ J. Gosset et al., Phys. Rev. C 16, (1977) 629; L. F. Oliveira, R. Donangelo, and J. O. Rasmussen, Phys. Rev. C 19 (1979) 826.
- ¹² J. Hufner, K. Schafer, and B. Schurmann, Phys. Rev. C 12 (1975) 1888; M. Bleszynski and C. Sander, Nucl. Phys. A326 (1979) 525.
- ¹³ L. W. Townsend, Can. J. Phys. 61 (1983) 93; L. W. Townsend, J. W. Wilson, and J. W. Norbury, ibid. 63 (1985) 135; L. W. Townsend, J. W. Wilson, F. A. Cucinotta, and J. W. Norbury, Phys. Rev. C 34 (1986) 1491.
- ¹⁴ S. H. Fricke, Ph.D. Thesis, University of Minnesota, 1985 (unpublished); B. F. Bayman, P. J. Ellis, S. Fricke, and Y. C. Tang, Phys. Rev. Lett. 53 (1984) 1322.
- ¹⁵ L. W. Townsend and J. W. Wilson, Health Phys. 54 (1988) 409.

- 16 F. P. Brady et al., Phys. Rev. Lett. 60 (1988) 1699.
- 17 J. W. Wilson and L. W. Townsend, Can. J. Phys. 59 (1981) 1569.
- 18 L. W. Townsend and J. W. Wilson, NASA Reference Publication No. RP-1134, May 1985.
- 19 P. M. Morse and H. Feshbach, Methods of Theoretical Physics, (Mc-Graw Hill, New York, 1953) Part I, pp. 349-356.
- 20 C. Y. Wong, in Proceedings of the 5th High Energy Heavy Ion Study, Lawrence Berkeley Laboratory, Report No. LBL-12652, 1981 (unpublished).
- 21 J. W. Wilson, L. W. Townsend, and F. F. Badavi, Nucl. Inst. & Meth. B18 (1987) 225.
- 22 J. P. Wefel et al., Bull. Am. Phys. Soc. 34 (1989) 1137.

Figure 1: Momentum transfer to the ^{16}O projectile, as a function of impact parameter, for 2.1 AGeV oxygen colliding with a beryllium target.

Figure 2: Target-averaged longitudinal momentum downshifts as a function of projectile fragment mass number for 2.1 AGeV ^{16}O colliding with Be, C, Al, Cu, Ag, and Pb targets. The experimental data, taken from reference 2, are averaged over isotopes for each fragment mass.

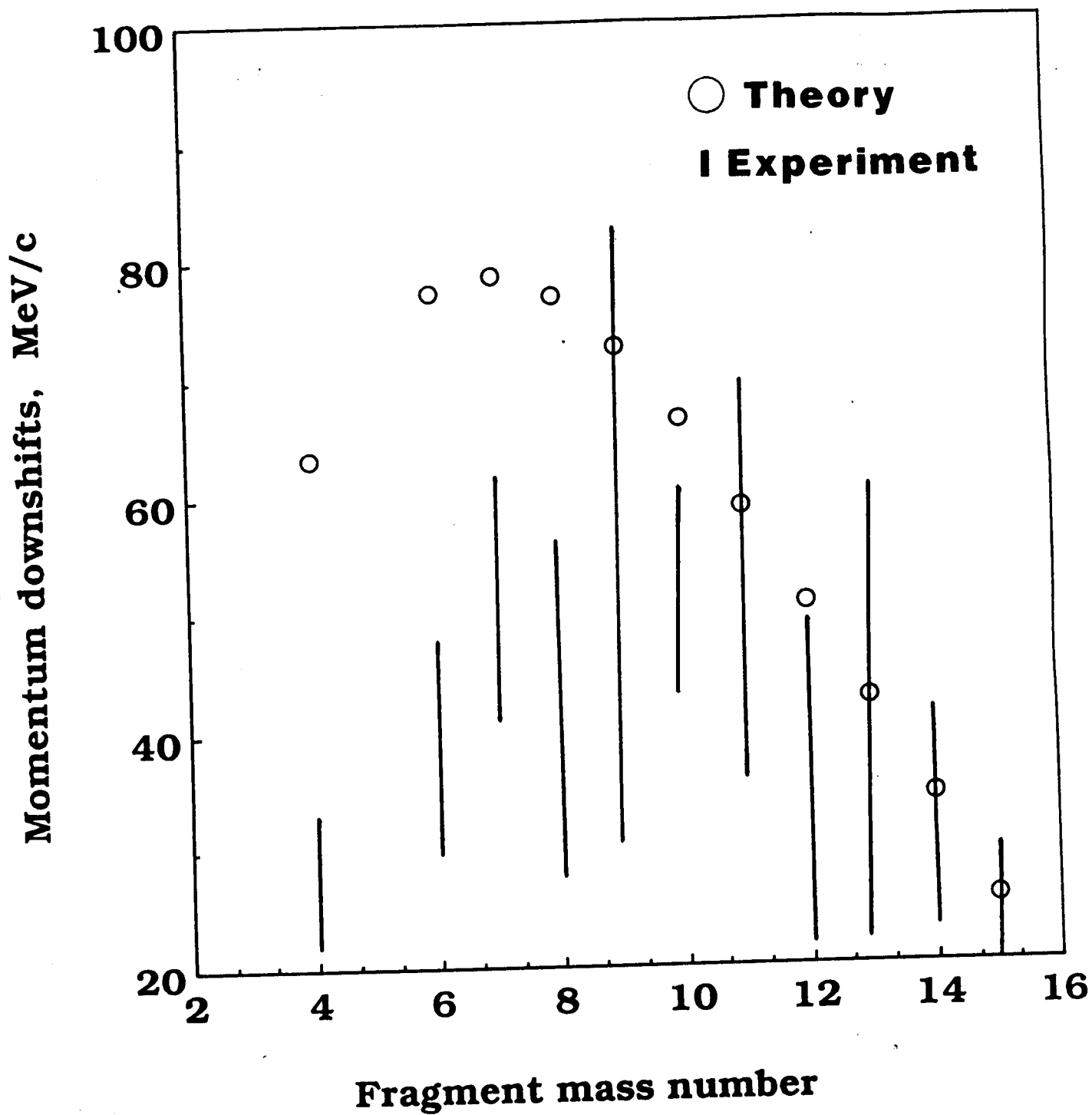
Figure 3: Transverse momentum widths as a function of fragment mass number for 1.2 AGeV ^{139}La colliding with a carbon target. The experimental data are taken from reference 16.



Khan/Khandelwal/Townsend/Wilson/Norbury

"An Optical Model Description of Momentum..

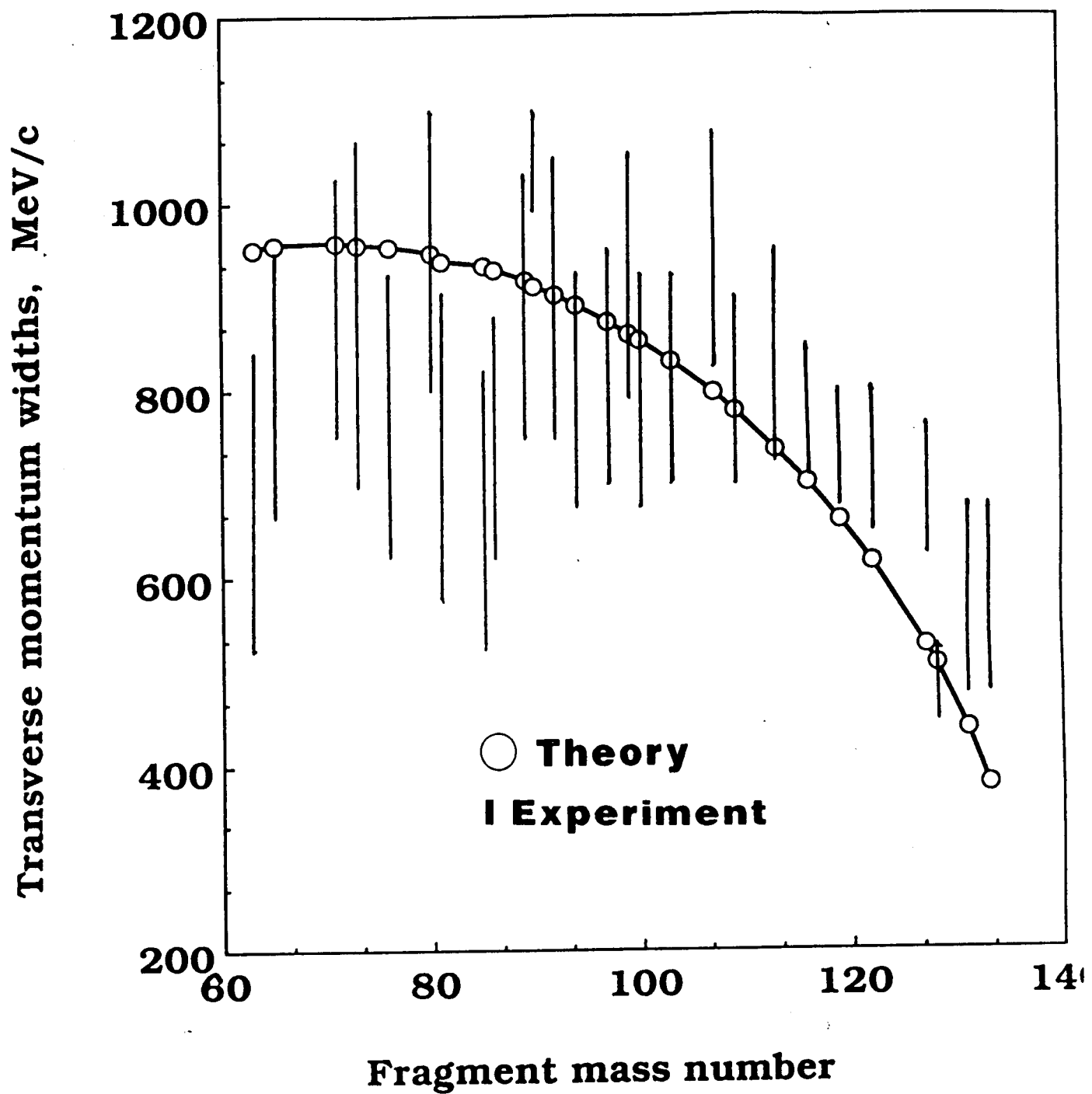
Figure 1.



Khan/Khandelwal/Townsend/Wilson/Norbury

"An Optical Model Description of Momentum..."

Figure 2.



Khan/Khandelwal/Townsend/Wilson/Norbury

"An Optical Model Description of Momentum...

Figure 3.